

# Optimizing the Radio Network Parameters of the Long Term Evolution System Using Taguchi's Method

Ahmad Awada, Bernhard Wegmann, Ingo Viering, *Member, IEEE*, and Anja Klein, *Member, IEEE*

**Abstract**—One of the primary aims of radio network planning is to configure the parameters of the base stations such that the deployment achieves the required quality of service. However, the adjustment of radio network parameters in a heterogeneous macro-only cellular network is a complex task, which involves a large number of configuration parameters with interactions among them. Existing commercial planning tools are based on local search methods, e.g., simulated annealing, that require problem-specific and heuristic definitions of the input parameters. The problem with local search methods is that their performance can significantly be degraded if the input parameters are misconfigured. To overcome these difficulties, an iterative optimization procedure based on Taguchi's method is proposed to find near-optimal settings. Taguchi's method was originally applied in manufacturing processes and has recently been used in several engineering fields. Unlike local search methods that heuristically discover the multidimensional parameter space of candidate solutions, Taguchi's method offers a scientifically disciplined methodology to explore the search space and select near-optimal values for the parameters. In this paper, the application of Taguchi's method in radio network optimization is illustrated by setting typical radio network parameters of the Long Term Evolution (LTE) system, i.e., the uplink power control parameters, antenna tilts, and azimuth orientations of trisectored macro base stations. Simulation results reveal that Taguchi's method is a promising approach for radio network optimization with respect to performance and computational complexity. It is shown that Taguchi's method has a comparable performance to simulated annealing in terms of power control and antenna azimuth optimizations; however, it performs better in terms of antenna tilt optimization. Moreover, it is presented that the performance of simulated annealing, as opposed to Taguchi's method, highly depends on the definition of the input parameters.

**Index Terms**—Antenna azimuth orientation, antenna tilt, radio network optimization, simulated annealing (SA), Taguchi's method (TM), uplink (UL) power control.

## I. INTRODUCTION

**I**N THE last few years, wireless communication has witnessed a remarkable growth, both in terms of mobile tech-

Manuscript received January 3, 2011; revised April 26, 2011 and June 24, 2011; accepted July 2, 2011. Date of publication July 25, 2011; date of current version October 20, 2011. The review of this paper was coordinated by Dr. N.-D. Dao.

A. Awada is with the Department of Communications Technology, Darmstadt University of Technology, 64289 Darmstadt, Germany.

B. Wegmann is with Nokia Siemens Networks, 81541 Munich, Germany.

I. Viering is with Normor Research GmbH, 81541 Munich, Germany.

A. Klein is with the Communications Engineering Laboratory, Darmstadt University of Technology, 64289 Darmstadt, Germany.

Color versions of one or more of the figures in this paper are available online at <http://ieeexplore.ieee.org>.

Digital Object Identifier 10.1109/TVT.2011.2163326

nologies and the number of subscribers. In 2011, it is expected that more than half of all communications will be carried out by mobile cellular networks [1]. This case has incited mobile operators and vendors to improve their radio network-planning services and provide more efficient optimization processes that aim at increasing the network capacity and coverage. A fundamental aspect of radio network planning is the configuration of the parameters that are associated with each base station, e.g., antenna tilts and angular settings. Due to the limited frequency reuse of modern cellular radio networks, the joint setting of the parameters of all cells with irregular layout and coverage areas becomes an important and challenging task. The number of cells determines the total number of parameters, each of them with a wide range of possible values. Hence, finding the optimal parameter setting for each base station that maximizes a predefined performance metric is a difficult problem.

Using a network-planning environment, we can manually select different parameter values for the base stations and, by experiments, determine their impacts on the network performance. Each experiment corresponds to a simulation run in the network-planning environment. Based on the results of the experiments, the value of each parameter can be tuned in favor of a better network performance. This process is then repeated until the network performance reaches a certain acceptance threshold. The major drawback of this trial-and-error approach is that it may not provide near-optimal solutions, because it is difficult to correctly adjust the parameters, particularly when the existing interactions among the parameters and their effects on the performance of the network cannot be taken into account. In addition, the number of experiments to be performed before a feasible solution of the problem is found can be quite large. Alternatively, if the parameters can take only discrete values, all possible combinations can be tested in a brute-force approach to select the optimal settings. The disadvantage of this method is that it is time consuming, because a very large number of experiments are required to be performed (NP-hard problem) and is therefore not viable in practice. Conventional radio network-planning tools use optimization methods based on local search such as simulated annealing (SA) [2], [3] and tabu search [4], [5]. These methods start from a candidate solution and then iteratively move to a neighbor solution by exploring new candidates in the neighborhood of the current solution. Other heuristic search methods such as the genetic algorithm can also be applied to radio network optimization [6]. While SA creates a new candidate solution by modifying the current solution with a local move, the genetic algorithm creates new

candidate solutions by combining two different solutions. The major drawback of these local search methods is that their performance highly depends on the heuristic definitions of the input parameters, i.e., parameters that should be initialized for the proper functioning of local search methods, e.g., the neighborhood structure of the current solution [7].

To overcome the aforementioned problems, Taguchi's method (TM) for experiment design is proposed to find radio network parameters that maximize a predefined performance metric. TM was first developed for the optimization of manufacturing processes [8] and then imported into several engineering fields, e.g., hardware design [9], power electronics [10]–[12], and microwave circuits [13]. Although very few applications of the method exist in communications [14], the method can be applied to solve other challenging optimization problems in this field. In this paper, the method is applied to radio network optimization within the scope of the Third-Generation Partnership Project Long-Term Evolution (3GPP LTE). The method uses the so-called orthogonal array (OA) [15], which should not be mixed up with an orthogonal antenna array. The OA was invented by Rao and was used by Genichi Taguchi to develop the base of what is currently known as TM. By using an OA, a reduced set of representative parameter combinations is selected to be tested from the full search space. The number of selected parameter combinations determines the number of experiments carried out and evaluated against a performance metric. Using all the experiments' results, a candidate solution is found, and the process is repeated until a desired criterion is fulfilled.

This paper is organized as follows. In Section II, the cellular network optimization problems in LTE are presented. The SA algorithm, which is used as a reference for comparison with TM, is briefly described in Section III. In Section IV, the optimization procedure based on TM is generalized to work for an arbitrary number of configuration parameters, and its application in network optimization is discussed. The system models of the LTE network in the uplink (UL) and downlink (DL) modes are described in Section V. Simulation results for the LTE network are presented in Section VI to compare TM with the SA algorithm. This paper is then concluded in Section VII.

## II. CELLULAR NETWORK OPTIMIZATION PROBLEMS IN LONG-TERM EVOLUTION

A cellular network consists of a large number of cells, and each cell  $c = 1, \dots, k$  underlies different radio conditions and capacity requirements that determine, for example, the cell range. The different characteristics of cells require cell-specific parameter settings that lead to an optimal overall network performance. In an LTE network, the following parameters typically require a cell-specific adaptation and optimization: 1) a UL power control parameter  $P_{0,c}$  that is used to control the signal-to-noise ratio (SNR) target of user equipment (UE) in cell  $c$  [16]; 2) the tilt  $\Theta_c$  of the transmit antenna serving cell  $c$ ; and 3) its azimuth orientation  $\Phi_c$ . These three parameters of each cell  $c$  need to be tuned so that the concerted operation of all cells leads to the optimal network performance.

In particular, the adoption of frequency reuse in LTE leads to strong interdependencies of neighboring cells and requires a joint optimization among the cells. Because the main aim of this paper is to investigate the feasibility of TM in radio network optimization, the simplest case will be considered, where one of the three parameters is jointly optimized for all cells, assuming that the other two parameters are fixed. For example,  $P_{0,c}$  is jointly optimized for all cells, assuming that the antenna azimuth orientations and tilts are fixed in the network. The joint optimization of different types of configuration parameters, e.g.,  $\Theta_c$  and  $\Phi_c$  for all cells, is briefly addressed in Section VII and will thoroughly be investigated in future work, because it requires some modifications on the proposed approach.

Let the variable  $x_c \in \{P_{0,c}, \Theta_c, \Phi_c\}$  designate one of the three configuration parameters for each cell  $c$ . In each optimization, only one type of configuration parameter is considered and jointly optimized for all cells; for example,  $x_c$  is  $P_{0,c}$ ,  $\Theta_c$ , or  $\Phi_c$  for all cells. Moreover, let  $\gamma_c$  be any performance metric for cell  $c$ . For example, the performance metric can be the mean, five percentile (5%-tile) or 50%-tile of the cumulative distribution function (CDF) of the UE throughput in a cell. Among all cells, there are interdependencies that need to be exploited and considered in the optimization. For example, adjusting the parameter  $x_j$  affects not only  $\gamma_j$  but also the performance metrics  $\gamma_{c \neq j}$  of all other cells. To account for these interactions, the performance metrics of all cells are bundled into one optimization function  $y(\gamma_1, \dots, \gamma_k)$ . Hence, the optimization problem is to jointly find the radio network parameters that maximize  $y(\gamma_1, \dots, \gamma_k)$  and is formulated as

$$\{x_1^{(\text{opt})}, \dots, x_k^{(\text{opt})}\} = \arg \max_{x_1, \dots, x_k} y(\gamma_1, \dots, \gamma_k). \quad (1)$$

The definition of the optimization function is typically problem specific and depends on the operator's policy. In this paper,  $\gamma_{c,p\%}$  is defined to be  $p\%$ -tile of the UE throughput distribution in a cell  $c$ , and to distinguish between the UL and the DL, the notations  $\gamma_{c,p\%} = \gamma_{c,p\%}^{(\text{UL})}$  in the UL and  $\gamma_{c,p\%} = \gamma_{c,p\%}^{(\text{DL})}$  in the DL are used. The value of  $p$  has a prominent role in steering the optimization toward cell coverage or capacity maximization. If a low value of  $p$  is chosen, e.g.,  $p = 5$ , more emphasis is given to the performance of cell-edge UEs, and the optimization primarily aims at increasing the cell coverage [17]. On the other hand, a high value of  $p$ , e.g., 50, lessens the impact of the performance of cell-edge UEs, and the optimization aims at maximizing the cell capacity. Different values for  $p$  are compared in Section VI.

According to the defined performance criterion, the aim is to maximize  $\gamma_{c,p\%}$  for each cell  $c$ . The intention of this optimization is to avoid solutions that improve the performance in some cells, at the expense of other cells. Thus, any cell  $c$  with a very low  $\gamma_{c,p\%}$  should render the value of the optimization function small, although there might be other cells with high performance. On the other hand, the optimization function should have a high value if each cell is performing, to some extent, as the other cells and all of these cells have high performance metrics.

Two averaging methods have been investigated as optimization functions. First, the arithmetic mean (AM) of  $\gamma_{c,p\%}$  would be applicable only if it is guaranteed that TM would not converge to a solution that improves the performance of the UEs in some cells and degrades the performance of other cells. However, because there is no routine in TM that checks for these undesired solutions, the algorithm would most probably converge to a solution that increases the mean of  $\gamma_{c,p\%}$ , which does not necessarily increase  $\gamma_{c,p\%}$  in every cell  $c$ . This case is because the AM alleviates the impact of a small  $\gamma_{c,p\%}$  in a cell  $c$  and aggravates the impact of large  $\gamma_{c,p\%}$ . To overcome this problem, the check for the aforementioned undesired solutions is implicitly done by changing the definition of the optimization function. In this paper, the harmonic mean (HM) is used instead of the AM. Unlike the AM, the HM aggravates the impact of small  $\gamma_{c,p\%}$  and lessens the impact of large  $\gamma_{c,p\%}$ . This case would guarantee, to some extent, that the algorithm converges to a solution that provides homogeneous user experience in all cells. Thus, the optimization function  $y(\gamma_{1,p\%}, \dots, \gamma_{k,p\%})$  is defined to be the HM of  $p\%$ -tile of the UE throughput distribution in a cell and is computed as

$$y(\gamma_{1,p\%}, \dots, \gamma_{k,p\%}) = \text{HM}(\gamma_{c,p\%}) = \frac{k}{\sum_{c=1}^k \frac{1}{\gamma_{c,p\%}}}. \quad (2)$$

Other optimization functions for network planning could also be used. One alternative would be to compute  $p\%$ -tile of the UE throughput distribution in the whole network rather than  $\gamma_{c,p\%}$  in each cell. Using other definitions for  $y$  does not affect TM or the SA algorithm, which work, in principle, regardless of the definition of the optimization function.

### III. OVERVIEW OF THE SIMULATED ANNEALING ALGORITHM

In this section, the application of SA algorithm in network optimization is briefly described. SA is a heuristic local search algorithm that has an explicit strategy to avoid the local maxima [18]. Unlike traditional local search methods such as the gradient ascent, which always moves in the direction of improvement, SA allows nonimproving moves to escape from the local maximum [19]. The probability of accepting a move that worsens the optimization function  $y$  is decreased during the search. The acceptance probability is controlled by the so-called temperature parameter  $T$  and the magnitude of the optimization function decrease  $\delta$  [18]. At a fixed temperature, the higher the difference  $\delta$ , the lower the probability to accept the move. Moreover, the higher the temperature  $T$ , the greater the acceptance probability. Let  $f(\mathbf{x})$  be the value of the optimization function  $y$  evaluated for  $\mathbf{x}$ , where  $\mathbf{x} = [x_1, x_2, \dots, x_k]$  is a vector that contains the configuration parameter  $x_c$  of each cell  $c$ . For example, if antenna tilt optimization is considered,  $\mathbf{x} = [\Theta_1, \Theta_2, \dots, \Theta_k]$ .

SA starts by selecting an initial candidate solution  $\mathbf{x} \in \Omega$ , where  $\Omega$  is the solution space defined as the set of all feasible candidate solutions. In each step, a new candidate  $\mathbf{x}'$  is generated from the neighborhood  $\mathcal{N}(\mathbf{x})$  of the current solution. If  $f(\mathbf{x}') \geq f(\mathbf{x})$ ,  $\mathbf{x}'$  is accepted as the current solution in the next

step; otherwise, it is accepted with some probability, depending on the parameters  $T$  and  $\delta = f(\mathbf{x}) - f(\mathbf{x}')$ . During the search, the temperature  $T$  is slowly decreased, and the process is repeated until the algorithm converges into a steady state. The steps of the SA algorithm are outlined in Pseudocode 1. Because SA is a heuristic search method, there are no general rules that guide the choice of the input parameters [2]. Therefore, decisions have to be made on the initial temperature  $T_0$ , the neighborhood structure  $\mathcal{N}(\mathbf{x})$ , and the temperature reduction function  $\rho(T)$ . In this paper, the initial temperature  $T_0$  is set such that a nonimproving move with a specific optimization function decrease  $\delta_{\max}$  is accepted in the beginning with a predefined probability  $\mu = \exp(-\delta_{\max}/T_0)$  [3]. As a result

$$T_0 = \frac{-\delta_{\max}}{\ln(\mu)} \quad (3)$$

where  $\ln(\cdot)$  is the natural logarithm operator. The neighborhood structure  $\mathcal{N}(\mathbf{x})$  is often defined as the set of candidate solutions that slightly differ from the current solution  $\mathbf{x}$  [20]. In this paper, a new candidate solution  $\mathbf{x}'$  is obtained by giving a small and random displacement  $\Delta$  for a randomly selected number  $n_{\text{disp}} = 1, \dots, k$  of configuration parameters in  $\mathbf{x}$  [21]. The displacement  $\Delta$  is generated by selecting a random number in the range  $(-\Delta_{\max}, +\Delta_{\max})$ , where  $\Delta_{\max}$  is the maximum displacement value. The value of the configuration parameter is also checked so that it is within the feasible set of values determined by the optimization range. For example, if  $n_{\text{disp}} = k$  and  $\Delta_{\max} = 1^\circ$  are selected in antenna tilt optimization,  $\mathbf{x}'$  is obtained by adding a random number between  $-1^\circ$  and  $+1^\circ$  to each tilt value in  $\mathbf{x}$ . To lower the temperature  $T$  every  $Q$  iterations, a standard geometric temperature reduction function is used, as shown in [2], i.e.,  $\rho(T) = \kappa \cdot T$ , where  $\kappa$  is a reduction ratio that is typically set between 0.8 and 0.99. Finally, the algorithm ends once the temperature has been reduced  $R$  times.

**Pseudocode 1:** SA with solution space  $\Omega$  and neighborhood structure  $\mathcal{N}(\mathbf{x})$  [18].

- 1: Select an initial solution  $\mathbf{x} = \mathbf{x}_0 \in \Omega$ .
- 2: Select an initial temperature  $T = T_0 > 0$ .
- 3: Select a neighborhood structure  $\mathcal{N}(\mathbf{x})$ .
- 4: Select a temperature reduction function  $\rho(T)$ .
- 5: Select the number  $Q$  of iterations executed at each temperature  $T$ .
- 6: Select the number of times  $R$  when the temperature is reduced.
- 7: Set the counter  $r$  of the number of times when the temperature is reduced to 0.
- 8: **repeat**
- 9:   Set the repetition counter  $q = 0$ .
- 10:   **repeat**
- 11:     Randomly generate  $\mathbf{x}' \in \mathcal{N}(\mathbf{x})$ .
- 12:     Compute  $\delta = f(\mathbf{x}) - f(\mathbf{x}')$ .
- 13:     **if**  $\delta \leq 0$  **then**
- 14:        $\mathbf{x} \leftarrow \mathbf{x}'$ .
- 15:     **else**
- 16:       Generate a random number  $n$  that is uniformly distributed between 0 and 1.

```

17:   if  $n < \exp(-\delta/T)$  then
18:      $x \leftarrow x'$ ;
19:   end if
20: end if
21:  $q \leftarrow q + 1$ .
22: until  $q = Q$ .
23:    $T \leftarrow \rho(T)$ .
24:    $r \leftarrow r + 1$ .
25: until  $r = R$ .
    
```

IV. OPTIMIZATION PROCEDURE BASED ON TAGUCHI'S METHOD

The newly proposed approach for radio network optimization is an iterative optimization procedure based on TM, which is introduced in [22]. In this section, the optimization procedure is generalized to work for a number  $k$  of configuration parameters that are determined by the number of cells of the network. The steps of this optimization procedure are depicted in Fig. 1 and discussed in detail in the following discussion.

A. Select the Proper OA

The first step in TM is to select the proper OA. Let  $s$  be the number of possible testing values for a parameter  $x_c$  and  $S = \{1, \dots, s\}$  be the set of index numbers for the testing values, also called a set of levels. For example, if a parameter  $x_c$  can take three values 5, 6, and 7, level 1 refers to value 5, level 2 refers to value 6, and level 3 refers to value 7. Each row  $i = 1, \dots, N$  of the OA, where  $N$  is the total number of rows, describes a possible combination of parameter levels to be tested in a corresponding experiment. Hence, an OA determines the testing level of each parameter in each experiment. To perform the experiments, each level of a parameter determined by the OA should be mapped to a corresponding testing value. The optimization function  $y(\gamma_{1,p\%}, \dots, \gamma_{k,p\%})$  is evaluated for each parameter combination determined by row  $i$  of the OA, resulting in a measured response  $y_i$ . In every iteration of the algorithm, the levels of each parameter are mapped to different testing values based on the candidate solution found in the previous iteration. Hence, a new set of  $N$  parameter combinations is tested in each iteration. The properties of the OA are described as follows.

By definition, an  $N \times k$  matrix  $P$ , having elements from  $S$ , is said to be an  $OA(N, k, s, t)$  with  $s$  levels, strength  $t$ , and index  $\lambda$  if every  $N \times t$  subarray of  $P$  contains each  $t$ -tuple based on  $S$  exactly  $\lambda$  times as a row [23]. Thus,  $\lambda$  denotes the number of times that each  $t$ -tuple based on  $S$  is tested. The higher the strength  $t$ , the more the OA considers the interactions among the configuration parameters. In mobile radio applications, the number  $k$  of configuration parameters that define the number of columns in the OA is determined by the number of cells of the radio network in question. Therefore, each column in the OA corresponds to a configuration parameter  $x_c$  of cell  $c$ . For example, if the antenna tilt optimization is considered, the first column corresponds to  $\Theta_1$ , the second column corresponds to  $\Theta_2$ , and so on. The same condition applies to  $P_{0,c}$  and  $\Phi_c$  optimizations. For illustration, one example of an  $OA(9, 4,$

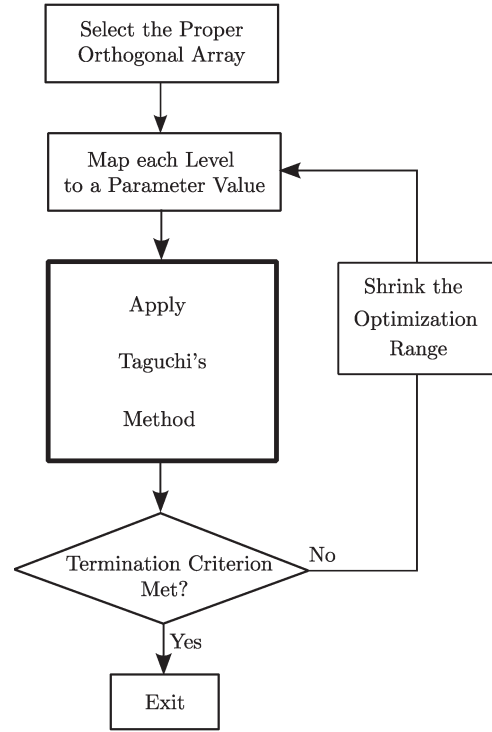


Fig. 1. Optimization procedure based on TM.

TABLE I  
ILLUSTRATIVE OA (9, 4, 3, 2) WITH THE MEASURED RESPONSES AND THEIR CORRESPONDING SN RATIOS

Experiment	$x_1$	$x_2$	$x_3$	$x_4$	Measured Response	SN Ratio
1	1	1	1	1	$y_1$	SN <sub>1</sub>
2	1	2	2	3	$y_2$	SN <sub>2</sub>
3	1	3	3	2	$y_3$	SN <sub>3</sub>
4	2	1	2	2	$y_4$	SN <sub>4</sub>
5	2	2	3	1	$y_5$	SN <sub>5</sub>
6	2	3	1	3	$y_6$	SN <sub>6</sub>
7	3	1	3	3	$y_7$	SN <sub>7</sub>
8	3	2	1	2	$y_8$	SN <sub>8</sub>
9	3	3	2	1	$y_9$	SN <sub>9</sub>

3, 2) with  $N = 9$ , which is nine times smaller than  $3^4 = 81$  possible combinations,  $k = 4$  configuration parameters,  $s = 3$  levels, and  $t = 2$  strength, is depicted in Table I. In any  $9 \times 2$  subarray of the OA in Table I, the nine-row combinations (1, 1), (1, 2), (1, 3), (2, 1), (2, 2), (2, 3), (3, 1), (3, 2), and (3, 3) are found, and each pair appears the same number of times, i.e.,  $\lambda = 1$ . In other words, every level of a parameter  $j$  is tested with every other level of a parameter  $c \neq j$  exactly  $\lambda = 1$  times. This property of the OA accounts for the interactions that might exist between the parameters. Therefore, the OA depicted in Table I analyzes not only the individual impact of each parameter on the performance but also the effect of any two parameters.

One basis property of the OA is that each parameter is tested at each level the same number of times. This case allows for a fair and balanced manner of testing the values of the parameters. In Table I, each level is tested three times for every parameter. Moreover, any subarray  $N \times k'$  of  $P$  is also an OA. Therefore, a new OA with a smaller number of configuration parameters can be obtained from an existing OA by removing one or more columns. This property is particularly useful when

the optimization problem has  $k' < k$  configuration parameters. In this case, an OA can directly be obtained from  $\mathbf{P}$  without the need to construct it.

Another fundamental issue is the construction and existence of an OA. Several techniques are known for constructing OAs based on Galois fields and finite geometries. More details about how an OA is constructed are found in [23]. In addition, it is not always possible to construct an OA with the desired number  $N$  of experiments. If the values of  $k$ ,  $s$ , and  $t$  are specified, there is a lower bound on the minimum number  $N$  of experiments so that an OA exists. Rao's bounds, as defined in [24] for an OA of strength 2 and 3, set a restriction on the number  $N$  of experiments and, therefore, the computational complexity of the algorithm. In principle,  $N$  is much smaller than the total number  $s^k$  of possible parameter combinations, i.e.,  $N \ll s^k$ . Several OAs with different numbers  $k$  of configuration parameters have been constructed and archived in the database maintained in [25]. Thus, the required OA can directly be selected from this database if found; otherwise, it needs to be constructed.

Having constructed an OA, the reduced set of representative parameter-level combinations is determined.

### B. Map Each Level to a Parameter Value

To conduct the experiments, the levels in the OA need to be mapped to parameter values; see Fig. 1. To this end, let  $\min_c$  and  $\max_c$  be the minimum and the maximum feasible values for parameter  $x_c$ , respectively,  $\ell \in \mathcal{S}$  be the level of a parameter value, and  $m$  be the index number of the iteration. In the first iteration  $m = 1$ , the center value of the optimization range for  $x_c$  is defined as

$$V_c^{(m)} = \frac{\min_c + \max_c}{2}. \quad (4)$$

In any iteration  $m$ , the level  $\ell = \lceil s/2 \rceil$  is always assigned to  $V_c^{(m)}$ . The other  $s - 1$  levels are distributed around  $V_c^{(m)}$  by adding or subtracting a multiple integer of step size  $\beta_c^{(m)}$ , which is defined in the first iteration  $m = 1$  as

$$\beta_c^{(m)} = \frac{\max_c - \min_c}{s + 1}. \quad (5)$$

In iteration  $m$ , the mapping function  $f_c^m(\ell)$  for a level  $\ell$  to a dedicated value of the parameter  $x_c$  can be described as follows:

$$f_c^m(\ell) = \begin{cases} V_c^{(m)} - (\lceil s/2 \rceil - \ell) \cdot \beta_c^{(m)}, & 1 \leq \ell \leq \lceil s/2 \rceil - 1 \\ V_c^{(m)}, & \ell = \lceil s/2 \rceil \\ V_c^{(m)} + (\ell - \lceil s/2 \rceil) \cdot \beta_c^{(m)}, & \lceil s/2 \rceil + 1 \leq \ell \leq s. \end{cases} \quad (6)$$

For example, consider an antenna tilt parameter  $x_1 = \Theta_1$  with a minimum value  $\min_1 = 0^\circ$  and a maximum  $\max_1 = 20^\circ$ . If  $x_1$  is tested with three levels, i.e.,  $s = 3$  and  $\mathcal{S} = \{1, 2, 3\}$ , level 2 is mapped in the first iteration to  $V_1^{(1)} = (0^\circ + 20^\circ)/2 = 10^\circ$ , level 1 is mapped to  $10^\circ - \beta_1^{(1)} = 5^\circ$ , and level 3 is mapped to  $10^\circ + \beta_1^{(1)} = 15^\circ$ . The values of  $V_c^{(m)}$  and  $\beta_c^{(m)}$  are updated at the end of each iteration if the termination criterion (see Section IV-E) is not met. This update

is necessary to test a new set of values in the following iterations and therefore cover the full optimization range of each parameter  $x_c$ .

### C. Apply TM

After conducting all the  $N$  experiments, TM converts the measured responses to so-called signal-to-noise (SN) ratios, which should not be confused with SNRs of the received signals. If the aim is to maximize the measured response  $y_i$ , the following definition of SN ratio applies for each experiment  $i$ :

$$\text{SN}_i = 10 \cdot \log_{10} (y_i^2) \text{ [dB]}. \quad (7)$$

$\text{SN}_i$  is referred to as the-larger-the-better ratio [26]. The higher the measured response  $y_i$ , the larger the ratio  $\text{SN}_i$ .

After computing  $\text{SN}_i$  for every experiment  $i$ , the average SN ratio is calculated for each parameter and level. The average SN ratio of  $x_c$  at level  $\ell$  is calculated as

$$\overline{\text{SN}}_{\ell,c} = \frac{s}{N} \sum_{i|\text{OA}(i,c)=\ell} \text{SN}_i \quad (8)$$

where  $\text{OA}(i, c)$  is the testing level of parameter  $x_c$  in experiment  $i$ . In the example in Table I, the average SN ratio  $\overline{\text{SN}}_{1,2}$  of parameter  $x_2$  at level 1 is computed by averaging (in decibels) over  $\text{SN}_1$ ,  $\text{SN}_4$ , and  $\text{SN}_7$ .

The best level  $\ell_{\text{best},c}$  for each parameter  $x_c$  is the level with the highest average SN ratio and is computed as

$$\ell_{\text{best},c} = \arg \max_{\ell} \overline{\text{SN}}_{\ell,c}. \quad (9)$$

According to the mapping function  $f_c^m(\ell)$ , the best settings for the configuration parameters in iteration  $m$  are derived. The best value of a parameter  $x_c$  found in iteration  $m$  is denoted by  $V_c^{(\text{best},m)}$ .

### D. Shrink the Optimization Range

At the end of each iteration, the termination criterion is checked. If it is not met, the best values found in iteration  $m$  are used as center values for the parameters in the next iteration  $m + 1$ , i.e.,

$$V_c^{(m+1)} = V_c^{(\text{best},m)}. \quad (10)$$

In iteration  $m + 1$ , the levels of each parameter  $x_c$  will be mapped to a different set of values, depending on  $V_c^{(m+1)}$ . It may happen that  $V_c^{(\text{best},m)}$  is close to  $\min_c$  or  $\max_c$ . As a result, the mapping function  $f_c^{m+1}(\ell)$  might assign a level  $\ell$  to a value that lies outside the optimization range defined by  $\min_c$  and  $\max_c$ . In this case, there is need for a procedure to consistently check if the mapped value is within the optimization range. For example, if  $f_c^{m+1}(1)$  is less than  $\min_c$ , the mapped values of levels 1 to  $\lceil s/2 \rceil - 1$  are distributed such that they are equally spaced between  $\min_c$  and  $V_c^{(m+1)}$ .

Moreover, the optimization range is reduced by multiplying the step size of each parameter  $x_c$  by a reduction factor  $\xi < 1$  as follows:

$$\beta_c^{(m+1)} = \xi \beta_c^{(m)}. \quad (11)$$

The value of  $\xi$  depends on the optimization problem considered. A high value of  $\xi$  makes the convergence of the algorithm slower; however, the parameters are tested, with more values rendering the optimization more accurate. On the other hand, a lower value of  $\xi$  shrinks the optimization range faster, at the expense of a possible degradation in performance, as the parameters are tested with a smaller number of possible values.

*E. Check the Termination Criterion*

With every iteration, the optimization range is reduced, and possible values of a parameter are closer to each other. Hence, the set that is used to select a near-optimal value for a parameter  $x_c$  becomes smaller. The optimization procedure terminates when all step sizes of the parameters are less than a predefined threshold  $\epsilon$ , i.e.,

$$\beta_c^{(m)} < \epsilon \forall c. \quad (12)$$

Different values of  $\epsilon$  are used for each optimization problem.

V. LONG-TERM EVOLUTION UPLINK AND DOWNLINK SYSTEM MODELS

In this section, the LTE UL and DL system models are presented, along with the simulation parameters. The optimizations are carried out offline in a network-planning environment. Therefore, a static system-level simulator is used to generate the results in the following discussion.

*A. General Definitions*

The following deployment scenario used in both UL and DL investigations is based on the model described in [27].

- The network has  $k = 33$  cells in a  $4 \times 4$  km (see Fig. 2), where every cell  $c$  is served by an enhanced Node B (eNodeB) located at position  $\vec{p}_c$ . This network layout has been proposed in [28]. Each eNodeB serves three cells, and all the transmit antennas of the eNodeBs are mounted at a height  $h_{BS}$ . Therefore, some sectors have the same eNodeB position due to sectorization.
- A UE  $u$  is located at a position  $\vec{q}_u$  on the ground, i.e., the UE height is zero. In the UL and DL modes, a 10-MHz system bandwidth with a total number of 50 physical resource blocks (PRBs) is considered for each sector  $c$ . The number of UEs is assumed to be 50 per cell, irrespective of the cell size. Moreover, a resource fair scheduler is assumed, where each UE is served by a single PRB.
- $k$  shadowing maps, which are denoted by  $M_c(\vec{q}_u)$  and are functions of a particular position of a UE in the network with respect to a cell  $c$ , are randomly generated from a log-normal distribution with zero mean and a standard deviation of 8 dB [29]. The shadowing maps of two cells are fully correlated if they are served by the same eNodeB;

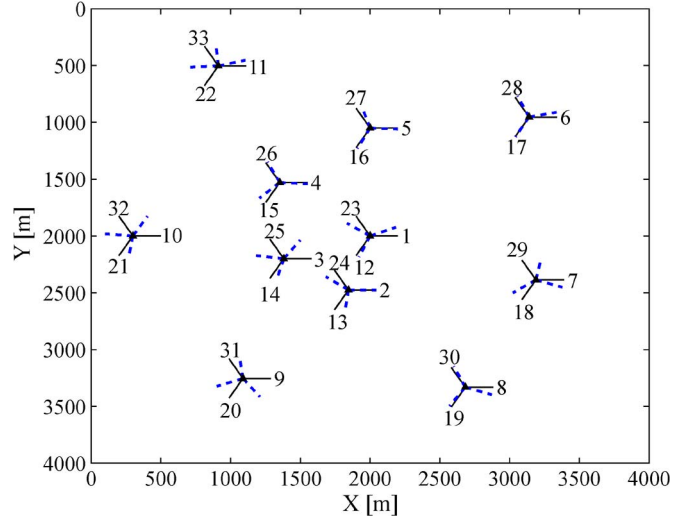


Fig. 2. Heterogeneous network with cells of different coverage areas. The default azimuth orientations of the antennas are shown in solid black lines, whereas the optimized orientations obtained by TM that applies  $HM(\gamma_{c,50\%}^{(DL)})$  as an optimization function are shown in dashed blue lines.

otherwise, they are correlated with coefficient 0.5. The decorrelation distance is assumed to be equal to  $d_s = 50$  m, i.e., two UEs have some correlation in the shadowing values if they are separated by a distance smaller than  $d_s$  [29].

- The path loss is a function of the distance  $d = |\vec{p}_c - \vec{q}_u|$  (in kilometers) between an eNodeB and a UE. It is given by

$$PL(d) = 148.1 + 37.6 \log_{10}(d) \quad (13)$$

assuming that all UEs have a penetration loss of 20 dB [29].

- The thermal noise power is  $N = -114$  dBm/PRB, including the noise figure.
- The transmit power  $P_{TX,c}^{(PRB)}$  per PRB of a sector  $c$  is 29 dBm.
- A 3-D antenna pattern is used. It is approximated using the model defined in [17] and [30] by summing up the azimuth and vertical patterns.
- An antenna gain  $A_{gain} = 14$  dBi is assumed for all sectors.

*B. Antenna Beam Patterns*

Let  $\Phi_c$ ,  $\Delta_\phi$ , and  $B_0$  denote the azimuth orientation of the antenna serving cell  $c$ , the azimuth beam width, and the maximum antenna backward attenuation, respectively. The azimuth pattern  $B_\phi(\Phi_c, \phi)$  of the antenna serving cell  $c$  is defined as in [17], i.e.,

$$B_\phi(\Phi_c, \phi) = -\min \left( B_0, 12 \cdot \left( \frac{\phi - \Phi_c}{\Delta_\phi} \right)^2 \right) \quad (14)$$

where the angle  $\phi = \angle(\vec{p}_c - \vec{q}_u)$ . The three-sector antennas of a single eNodeB have the default azimuth orientations  $\Phi_c \in \{0, 120^\circ, -120^\circ\}$ .

Similarly, let  $\Theta_c$  and  $\Delta_\theta$  denote the tilt of the antenna serving cell  $c$  and the elevation beam width, respectively. The vertical pattern  $B_\theta(\Theta_c, \theta)$  of the antenna is given by

$$B_\theta(\Theta_c, \theta) = -\min \left( B_0, 12 \cdot \left( \frac{\theta - \Theta_c}{\Delta_\theta} \right)^2 \right) \quad (15)$$

where the angle  $\theta = \arctan(h_{BS}/|\vec{p}_c - \vec{q}_u|)$ . The azimuth and the elevation patterns have the same backward attenuation  $B_0$ . In this paper,  $\Delta_\phi$ ,  $\Delta_\theta$ , and  $B_0$  are set to  $70^\circ$ ,  $9^\circ$ , and 25 dB, respectively.

The 3-D pattern of the antenna in sector  $c$  can now be written as a sum of the two aforementioned patterns as

$$B(\Phi_c, \phi, \Theta_c, \theta) = -\min \left\{ - (B_\phi(\Phi_c, \phi) + B_\theta(\Theta_c, \theta)), B_0 \right\}. \quad (16)$$

Having defined the path-loss function, shadowing, and antenna beam patterns, the overall signal attenuation  $L_c(d, \vec{q}_u, \Phi_c, \Theta_c)$  of a UE  $u$ , located at position  $\vec{q}_u$  with respect to a cell  $c$  is computed as

$$L_c(d, \vec{q}_u, \Phi_c, \Theta_c) = PL(d) - A_{\text{gain}} - B(\Phi_c, \phi, \Theta_c, \theta) + M_c(\vec{q}_u). \quad (17)$$

Moreover, each UE  $u$  in the network is served by a cell  $c = X(u)$ , where  $X(u)$  is the connection function that assigns a UE  $u$  to a single cell  $c$ . The connection function is determined by selecting the cell whose reference signal received power (RSRP) level measured by a UE in DL transmission is the strongest [31], [32] without considering any hysteresis value.

### C. UL Power Control

The UL power control in LTE is composed of an open-loop component that compensates for long-term channel variations such as path loss and shadowing and another closed-loop correction term that accounts for the errors in the UE path-loss estimates [33]. The performance of UL open- and closed-power control is discussed in detail in [34]–[37]. In this paper, only the open-loop component is considered, and the closed-loop term is neglected. This case is because the open-loop power control is necessary for proper network performance, whereas the closed-loop term is optional. As a result, the setting of the total transmit power  $P_{\text{TX},u}^{(\text{Total})}$  for the physical uplink shared channel (PUSCH) transmission of a UE  $u$  connected to a cell  $c$  simplifies to

$$P_{\text{TX},u}^{(\text{Total})} = \min (P_{\text{max}}, P_{0,c} + \alpha_c \cdot L_c(d, \vec{q}_u, \Phi_c, \Theta_c) + 10 \cdot \log_{10}(M_u)) \quad (18)$$

where  $P_{\text{max}}$  is the maximum configured transmission power of a UE,  $P_{0,c}$  is a parameter that is used to control the SNR target of the UEs connected to a cell  $c$ ,  $\alpha_c \in \{0, 0.4, 0.5, 0.6, 0.7, 0.8, 0.9, 1\}$  is a cell-specific path-loss compensation coefficient, and  $M_u$  is the number of PRBs allocated by a scheduler to a UE  $u$ . The default value of  $P_{\text{max}}$  used in the simulation results is 23 dBm for all UEs.

Because each UE is served by a single PRB, the transmit power per PRB of a UE  $u$ , which is denoted by  $P_{\text{TX},u}^{(\text{PRB})}$ , is computed by setting  $M_u$  to 1, thus resulting in

$$P_{\text{TX},u}^{(\text{PRB})} = \min (P_{\text{max}}, P_{0,c} + \alpha_c \cdot L_c(d, \vec{q}_u, \Phi_c, \Theta_c)). \quad (19)$$

### D. Signal-to-Interference-Plus-Noise Ratio (SINR) and UE Throughput in the UL

The received power of a UE  $u$ , which is served by a cell  $c$ , is calculated as

$$P_{\text{RX},u} = P_{\text{TX},u}^{(\text{PRB})} - L_c(d, \vec{q}_u, \Phi_c, \Theta_c). \quad (20)$$

The interference that a UE  $u$  would produce at any other cell  $j \neq c$  is defined as

$$I_{j,u} = P_{\text{TX},u}^{(\text{PRB})} - L_j(d, \vec{q}_u, \Phi_j, \Theta_j). \quad (21)$$

This interference is only generated if the serving cell  $c$  schedules a UE  $u$  at the PRB and time of interest. Thus, the interference produced by the UEs of cell  $j$  to a target cell  $c$ , denoted by  $I_{c,j}$ , is a random variable that depends on the scheduling probabilities of the UEs in cell  $j$ . Let  $P_{\text{RX},u}^{(\text{lin})}$ ,  $I_{c,j}^{(\text{lin})}$  and  $N^{(\text{lin})}$  designate the linear forms of  $P_{\text{RX},u}$ ,  $I_{c,j}$ , and  $N$ , respectively. In this paper, the average of the SINR of a UE  $u$ , which is served by a cell  $c$ , is considered and defined as

$$\begin{aligned} \text{SINR}_u^{(\text{UL})} &= E \left[ \frac{P_{\text{RX},u}^{(\text{lin})}}{N^{(\text{lin})} + \sum_{j \neq c} I_{c,j}^{(\text{lin})}} \right] \\ &= P_{\text{RX},u}^{(\text{lin})} \cdot E \left[ \frac{1}{N^{(\text{lin})} + \sum_{j \neq c} I_{c,j}^{(\text{lin})}} \right]. \quad (22) \end{aligned}$$

To compute the expected value of the SINR, it is assumed that there exists a UE in each cell  $j \neq c$  that is scheduled at the same PRB and time of interest. However, the interferer in each cell  $j$  can be any of the connected UEs. To have a good approximation of the interference, Monte Carlo integration is followed, where  $N_S = 10\,000$  random  $k$ -tuples, containing samples of interferers from each cell  $j$ , are generated. The interference signals that are induced by all UEs of cells  $j \neq c$  are summed up using a  $k$ -tuple, and the inner term of the expectation is averaged over  $N_S$   $k$ -tuples. More details about the computation of the expectation term are found in [16].

After defining the SINR, the UL throughput  $R_u^{(\text{UL})}$  of a UE  $u$  is computed using an approximation based on the Shannon capacity formula as

$$R_u^{(\text{UL})} = W_{\text{eff}} \cdot B \cdot \log_2 \left( 1 + \frac{\text{SINR}_u^{(\text{UL})}}{S_{\text{eff}}} \right) \quad (23)$$

where  $W_{\text{eff}} = 0.88$  and  $S_{\text{eff}} = 1.25$  are the bandwidth and SINR efficiency factors [38], respectively, and  $B = 180$  kHz is the bandwidth that is occupied by one PRB.

### E. SINR and UE Throughput in the DL

In the DL, the received power  $P_{c,u}$  of a UE  $u$  served by a sector  $c$  can now be expressed as

$$P_{c,u} = P_{\text{TX},c}^{(\text{PRB})} - L_c(d, \vec{q}_u, \Phi_c, \Theta_c). \quad (24)$$

A UE  $u$  has not only  $P_{c,u}$  from the serving cell  $c$  but also received powers from other cells  $j \neq c$  defined as

$$P_{j,u} = P_{\text{TX},j}^{(\text{PRB})} - L_j(d, \vec{q}_u, \Phi_j, \Theta_j). \quad (25)$$

The respective sum of these received powers constitutes the total generated interference. The most influential interferers are the neighboring cells, because they have the strongest received power levels. The SINR of a UE  $u$  in the DL can now be computed as

$$\text{SINR}_u^{(\text{DL})} = \frac{P_{c,u}^{(\text{lin})}}{N^{(\text{lin})} + \sum_{j \neq c} P_{j,u}^{(\text{lin})}} \quad (26)$$

where  $P_{c,u}^{(\text{lin})}$  is the linear form of  $P_{c,u}$ . The DL throughput of a UE  $u$ , which is denoted by  $R_u^{(\text{DL})}$ , is computed as in (23).

## VI. SIMULATION RESULTS

In this section, the deployment scenario in Fig. 2 is optimized in terms of tuning the parameters  $x_c \in \{P_{0,c}, \Theta_c, \Phi_c\}$  for all  $k = 33$  cells using the optimization procedure based on TM and the SA algorithm. Each type of configuration parameter is jointly optimized for all cells, assuming that the other two parameters are fixed. Because there are 33 parameters to optimize, the OA to be selected for TM should have 33 columns. Moreover, to efficiently explore the search space, each parameter should be tested in each iteration with a relatively high number of values. For these reasons, the OA that is used in this paper is OA(512, 33, 16, 2) and can be found in the database maintained in [25]. This OA allows the testing of  $s = 16$  different values for each parameter  $x_c$  in every iteration. In addition, it has a strength of  $t = 2$ , which is necessary to account for the interactions that exist between any two parameters.

### A. Evaluation Methodology

TM and SA are compared with respect to performance and computational complexity. Both algorithms are run using the same optimization function  $y$  defined in (2), and the cell performance  $\gamma_{c,p\%}$  is evaluated for three different values of  $p$ , i.e.,  $p = 5, 10$  and  $50$ . For example, if  $p = 5$  is used, the optimization function  $y$  is the HM of 5%-tile of the UE throughput distribution in a cell and is denoted by  $y = \text{HM}(\gamma_{c,5\%}^{(\text{DL})})$  in the DL and  $\text{HM}(\gamma_{c,5\%}^{(\text{UL})})$  in the UL. The parameter configurations obtained by both algorithms in each optimization problem are evaluated using the following two performance criteria: 1) the cell coverage reflected by the CDF of 5%-tile of the UE throughput distribution in a cell  $c$ , which is denoted by  $\gamma_{c,5\%}^{(\text{DL})}$  in the DL and  $\gamma_{c,5\%}^{(\text{UL})}$  in the UL, and 2) the cell capacity reflected by the CDF of 50%-tile of the UE throughput distribution in a

cell  $c$ , which is denoted by  $\gamma_{c,50\%}^{(\text{DL})}$  in the DL and  $\gamma_{c,50\%}^{(\text{UL})}$  in the UL.

The criterion that is used for complexity evaluation is the number of times that the optimization function  $y$  is evaluated, which has been referred to as the number of experiments. In case of TM,  $N$  experiments are performed in each iteration, and the algorithm terminates after a predefined number  $M$  of iterations. As a result, the total number of experiments performed by TM is  $N \cdot M$ . Note that TM does not have an initial solution  $\mathbf{x}_0$  and generates a new candidate solution every  $N$  experiments. The lower the number  $N$  of rows in the OA, the lower the complexity of the algorithm. Similarly, SA evaluates the optimization function  $Q$  times in the inner loop of Pseudocode 1, i.e., lines 9 and 21, and this process is repeated  $R$  times in the outer loop defined in lines 7 and 24. Therefore, the total number of experiments evaluated by SA is  $Q \cdot R$ .

To have a fair performance comparison between the two algorithms, the same complexity is applied: TM and SA are run for the same number of experiments, and the performance of their optimized parameter settings obtained at the end of the simulation is compared. To this end, the termination criterion  $\epsilon$  of TM is set such that  $M$  iterations are performed in total. Having determined  $N$  and  $M$  and decided on a predefined value for  $Q$ , the number of iterations  $R$  in SA can simply be computed as

$$R = \frac{N \cdot M}{Q}. \quad (27)$$

To check the convergence time of each algorithm, the value of  $y$  is plotted as a function of the number of experiments.

### B. Input Parameters of the Algorithms

The input parameters of TM and the SA algorithm used in the three optimizations are summarized in Table II. The parameters  $\delta_{\max}$ ,  $\kappa$ , and  $Q$  of SA are selected after some experimentation, because there are no clear rules that guide their choice [2]. Note also that the proper input parameter setting of SA is not straightforward and is even differentiated between various optimization functions. For example, a degradation of  $\delta_{\max} = 1$  kbps in the value of the optimization function is initially allowed for  $\text{HM}(\gamma_{c,5\%})$ , whereas  $\delta_{\max} = 5$  kbps for  $\text{HM}(\gamma_{c,50\%})$ .

The performance of SA highly depends on the definition of the neighborhood structure  $\mathcal{N}(\mathbf{x})$  determined by the 2-tuple  $(n_{\text{disp}}, \Delta_{\max})$  [7]. Therefore, SA might not provide an acceptable performance from the first trial if  $\mathcal{N}(\mathbf{x})$  is misconfigured. For this reason, SA is run multiple times with different  $\mathcal{N}(\mathbf{x})$  definitions and is compared with TM. The neighborhood structures used by SA are shown in Table III, which presents the values of the 2-tuple  $(n_{\text{disp}}, \Delta_{\max})$  for each tuple. Note that the neighborhood structure  $\mathcal{N}_C$  is not used in  $\Theta_c$  and  $\Phi_c$  optimizations, because it did not yield a fast convergence or noteworthy performance improvement compared to  $\mathcal{N}_A$  and  $\mathcal{N}_B$  in  $P_{0,c}$  optimization.

In the remainder of this paper, the following notations are used: 1)  $\text{TM}(\gamma_{c,p\%}^{(\text{UL}/\text{DL})})$  denotes TM, which applies

TABLE II  
INPUT PARAMETERS OF TM AND THE SA ALGORITHM IN EACH OF THE THREE OPTIMIZATION PROBLEMS. IN THE CASE OF SA,  
THE PARAMETERS ARE EVEN DIFFERENTIATED BETWEEN VARIOUS OPTIMIZATION FUNCTIONS

Taguchi's Method						
Parameter	$P_{0,c}$ Optimization		$\Theta_c$ Optimization		$\Phi_c$ Optimization	
$\epsilon$	0.06 dB		0.02°		0.01°	
$\xi$	0.8		0.8		0.8	
$N$	512 experiments		512 experiments		512 experiments	
$M$	15 iterations		20 iterations		30 iterations	
$N \cdot M$	7680 experiments		10240 experiments		15360 experiments	
Simulated Annealing						
Parameter	$P_{0,c}$ Optimization		$\Theta_c$ Optimization		$\Phi_c$ Optimization	
	HM( $\gamma_{c,5\%}^{(UL)}$ )	HM( $\gamma_{c,50\%}^{(UL)}$ )	HM( $\gamma_{c,5\%}^{(DL)}$ )	HM( $\gamma_{c,50\%}^{(DL)}$ )	HM( $\gamma_{c,5\%}^{(DL)}$ )	HM( $\gamma_{c,50\%}^{(DL)}$ )
$\mu$	0.5		0.5		0.5	
$\delta_{\max}$	1 kbps	5 kbps	1 kbps	5 kbps	1 kbps	5 kbps
$T_0$	1.4427	7.2135	1.4427	7.2135	1.4427	7.2135
$\kappa$	0.95		0.95		0.95	
$Q$	32 experiments		32 experiments		32 experiments	
$R$	240 iterations		320 iterations		480 iterations	
$Q \cdot R$	7680 experiments		10240 experiments		15360 experiments	

TABLE III  
VALUES OF 2-TUPLE ( $n_{\text{disp}}, \Delta_{\max}$ ) FOR EACH NEIGHBORHOOD STRUCTURE USED BY SA IN EACH OPTIMIZATION PROBLEM

$\mathcal{N}(\mathbf{x})$ Definition	$P_{0,c}$ Optimization	$\Theta_c$ Optimization	$\Phi_c$ Optimization
$N_A$	(33, 1 dB)	(33, 1°)	(33, 1°)
$N_B$	(33, 3 dB)	(33, 3°)	(33, 3°)
$N_C$	(1, 1 dB)	-	-

the HM of  $\gamma_{c,p\%}^{(UL/DL)}$  as an optimization function and 2) SA( $\gamma_{c,p\%}^{(UL/DL)}$ ,  $\mathbf{x}_0, \mathcal{N}(\mathbf{x})$ ) refers to SA, which applies the HM of  $\gamma_{c,p\%}^{(UL/DL)}$  as an optimization function,  $\mathbf{x}_0$  as an initial candidate solution, and  $\mathcal{N}(\mathbf{x}) = \{N_A, N_B, N_C\}$  as a neighborhood structure. For example, the notation SA( $\gamma_{c,5\%}^{(UL)}$ ,  $-65$  dBm,  $N_A$ ) refers to SA, which applies the HM of  $\gamma_{c,5\%}^{(UL)}$  as an optimization function,  $-65$  dBm for each  $P_{0,c}$  as an initial solution, i.e.,  $\mathbf{x}_0 = -65$  dBm  $\forall c$ , and  $N_A$  as a neighborhood structure.

### C. $P_0$ Optimization in a Heterogeneous Network

The key motivation for power control is to avoid a very large dynamic range (DR) of the received signal power values among all UEs that are connected to the same eNodeB rather than to mitigate intercell interference [32]. This case is because a large DR reduces the orthogonality in a single-carrier frequency-division multiple access (SC-FDMA) radio system and introduces intracell interference, which, in turn, decreases the throughputs of the UEs [39]. In this paper, the DR of each cell is measured in decibels as the difference between 5%-tile and 95%-tile of the CDF of the UE received signal power. The optimization range of  $P_{0,c}$  for a cell  $c$  is selected such that the DR does not exceed a predefined threshold set to 25 dB. To this end,  $P_0$  is swept from  $-70$  dBm to  $-50$  dBm for each cell in the network, whereas the path-loss coefficient  $\alpha_c$  based on (18) is assumed to be fixed, i.e.,  $\alpha_c = 0.6$ . The  $P_0$  value that does not exceed a DR threshold of 25 dB is selected to be the maximum value of the optimization range for each parameter  $x_c$ , i.e.,  $\max_c$ . The lower bound of the optimization range is assumed to be  $-70$  dBm for all cells, i.e.,  $\min_c = -70$  dBm  $\forall c$ .

As aforementioned, the other two configuration parameters  $\Theta_c$  and  $\Phi_c$  are kept fixed. The antenna azimuth orientations

are assumed to have the default values, as given in Fig. 2, and the impact of elevation is not considered, i.e.,  $h_{BS} = 0$  and  $\Theta_c = 0 \forall c$ . In addition to SA, the performance of TM is compared to the performance of the so-called 95%-tile rule [16]. The definition of the 95%-tile rule is to have 5%-tile of the edge users in each cell transmitting at full power  $P_{\max}$  as a means of compensating for their large path-loss attenuation. To have 5% of the UEs in power limitation,  $P_{0,c}$  of a cell  $c$  is computed as

$$P_{0,c} = P_{\max} - \alpha_c \cdot L_{c,95\%-\text{tile}} \quad (28)$$

where  $L_{c,95\%-\text{tile}}$  is 95%-tile of the UE overall signal attenuation distribution in a cell  $c$ .

The convergence curves of TM and SA that apply HMs of  $\gamma_{c,5\%}^{(UL)}$  and  $\gamma_{c,50\%}^{(UL)}$  are shown in Figs. 3 and 4, respectively. It can be noticed from both figures that the initial solution  $\mathbf{x}_0$  affects the convergence rate of the SA that applies  $N_A$  at the beginning of the simulation run but does not have a significant impact on the converged value of the optimization function. The main reason for this is that nonimproving moves are allowed, which makes SA less dependent on the initial solution.

In Fig. 3, the SA that applies  $N_C$  has a slower convergence rate than its counterpart, which applies  $N_A$ ; however, the latter approach converges to a slightly lower value than the former approach. In contrast, the SA that applies  $N_C$  in Fig. 4 has a slower convergence rate than its counterpart, which applies  $N_A$  or  $N_B$  and even converges to a lower value. Thus, the performance of SA highly depends on the heuristic definition of the neighborhood structure  $\mathcal{N}(\mathbf{x})$ . Finding a good definition for the neighborhood structure is cumbersome, and we may need to try different neighborhood structures to get an acceptable result. If compared with SA, TM converges to slightly higher values of the optimization function in both figures. In Fig. 3, TM also

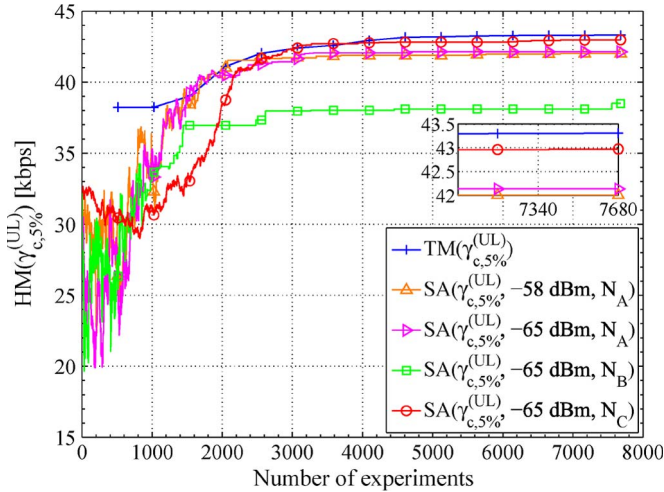


Fig. 3. HM of  $\gamma_{c,5\%}^{(UL)}$  as a function of the number of experiments for TM and SA indicated by  $SA(\gamma_{c,5\%}^{(UL)}, \mathbf{x}_0, \mathcal{N}(\mathbf{x}))$ , with  $P_{0,c}$  as a configuration parameter.

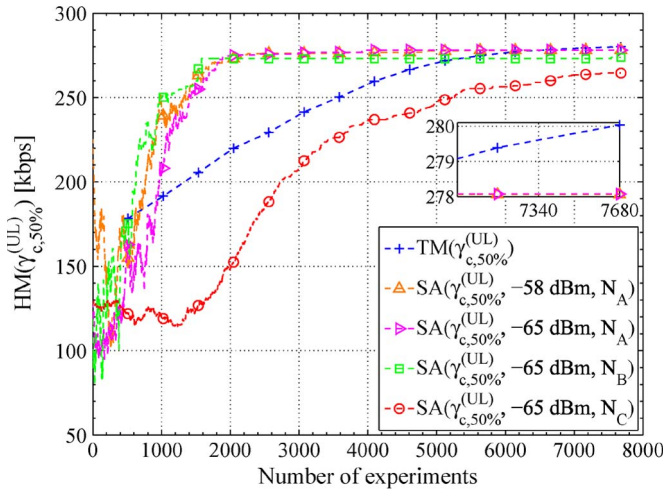


Fig. 4. HM of  $\gamma_{c,50\%}^{(UL)}$  as a function of the number of experiments for TM and SA indicated by  $SA(\gamma_{c,50\%}^{(UL)}, \mathbf{x}_0, \mathcal{N}(\mathbf{x}))$ , with  $P_{0,c}$  as a configuration parameter.

has a faster convergence rate than SA at the beginning of the simulation run, whereas in Fig. 4, it has a slower convergence rate than the SA that applies  $N_A$  or  $N_B$  and is faster than the SA that applies  $N_C$ .

The rounded settings of  $P_{0,c}$  are plotted as a function of  $L_{c,95\%-\text{tile}}$  in Fig. 5 for the 95%-tile rule, TM, and SA evaluated using the HM of  $\gamma_{c,5\%}^{(UL)}$  as an optimization function. Based on the figure, it can be observed, for all the three methods, that the  $P_{0,c}$  of the cells with higher  $L_{c,95\%-\text{tile}}$  are smaller in general than cells with lower  $L_{c,95\%-\text{tile}}$ . In other words, cells that cover large areas use lower  $P_{0,c}$  values than cells that cover smaller areas. Moreover, most of the  $P_{0,c}$  values obtained by TM are equal to the values of SA and the 95%-tile rule.

The CDF's of  $\gamma_{c,5\%}^{(UL)}$  and  $\gamma_{c,50\%}^{(UL)}$  are shown in Figs. 6 and 7, respectively, for the 95%-tile rule, TM, and SA evaluated using the neighborhood structures, yielding the best performance. In both figures, it can be noticed that the performance of TM and

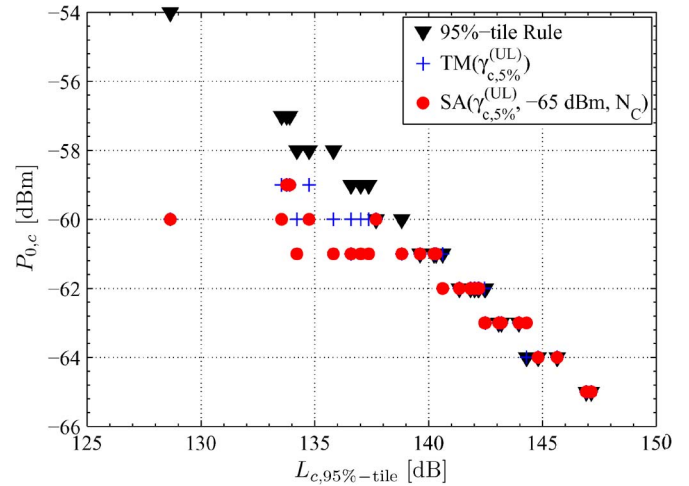


Fig. 5.  $P_{0,c}$  as a function of  $L_{c,95\%-\text{tile}}$  for the 95%-tile rule, TM, and SA indicated by  $SA(\gamma_{c,5\%}^{(UL)}, \mathbf{x}_0, \mathcal{N}(\mathbf{x}))$ .

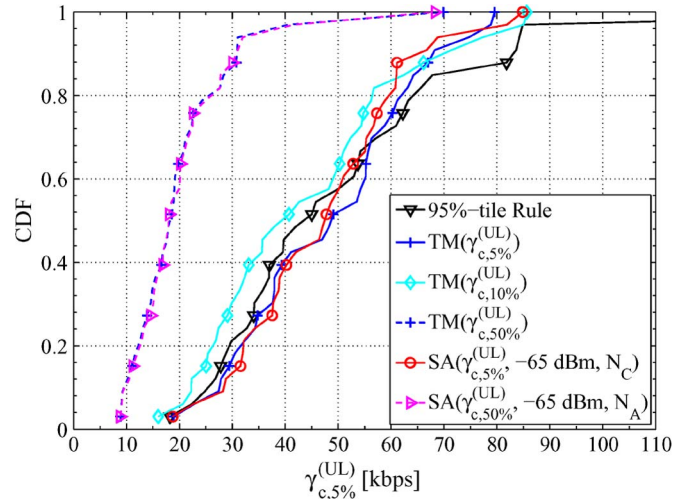


Fig. 6. CDFs of  $\gamma_{c,5\%}^{(UL)}$  obtained from applying the 95%-tile rule, TM, and SA indicated by  $SA(\gamma_{c,p\%}^{(UL)}, \mathbf{x}_0, \mathcal{N}(\mathbf{x}))$ , with  $P_{0,c}$  as a configuration parameter.

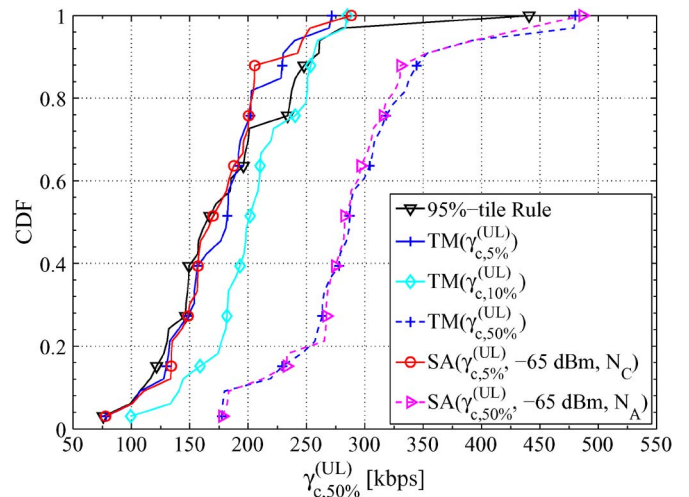


Fig. 7. CDFs of  $\gamma_{c,50\%}^{(UL)}$  obtained from applying the 95%-tile rule, TM, and SA indicated by  $SA(\gamma_{c,p\%}^{(UL)}, \mathbf{x}_0, \mathcal{N}(\mathbf{x}))$ , with  $P_{0,c}$  as a configuration parameter.

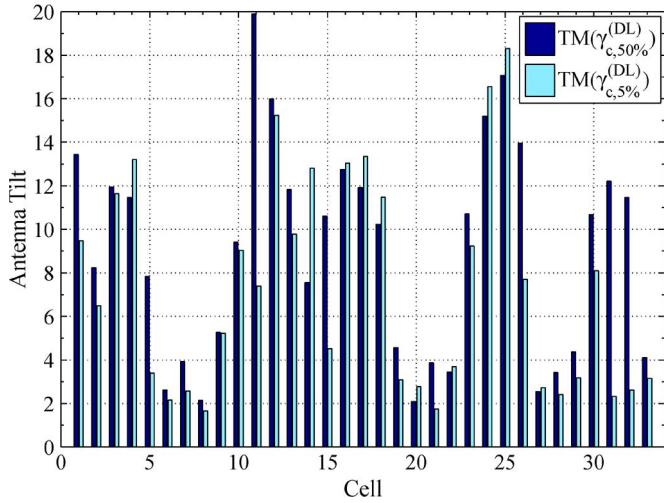


Fig. 8. Settings of the antenna tilts obtained by TM that applies HMs of  $\gamma_{c,50\%}^{(DL)}$  and  $\gamma_{c,5\%}^{(DL)}$  as optimization functions.

SA depends on the optimization function used. In Fig. 6, TM that applies the HM of  $\gamma_{c,5\%}^{(UL)}$  as an optimization function has a better coverage performance than approaches that apply the HM of  $\gamma_{c,10\%}^{(UL)}$  or  $\gamma_{c,50\%}^{(UL)}$ . However, TM that applies the HM of  $\gamma_{c,5\%}^{(UL)}$  has lower median UE throughputs compared to approaches that apply the HM of  $\gamma_{c,10\%}^{(UL)}$  or  $\gamma_{c,50\%}^{(UL)}$  in Fig. 7. Note that the  $\gamma_{c,10\%}^{(UL)}$  metric achieves, among others, the best tradeoff between cell-edge and median UE throughputs. Moreover, TM achieves a slightly better performance than the 95%-tile rule and SA evaluated with the same optimization function.

#### D. Optimization of the Antenna Tilts in a Heterogeneous Network

In this section, the antenna tilts are optimized by TM and SA for various optimization functions. The antenna azimuth orientations are assumed to have default values, as given in Fig. 2. The height of the eNodeB is assumed to be 30 m, i.e.,  $h_{BS} = 30$  m, and the optimization range for tilt  $\Theta_c$  of a transmit antenna of cell  $c$  is set between  $\min_c = 0^\circ$  and  $\max_c = 20^\circ$ . The optimized antenna tilts for each cell obtained by TM are shown in Fig. 8 for two different performance metrics. According to the figure, 23 out of 33 sectors have smaller tilt values when the HM of  $\gamma_{c,5\%}^{(DL)}$  is used instead of the HM of  $\gamma_{c,50\%}^{(DL)}$ . Maximizing the cell coverage requires smaller tilt values to increase the throughputs of cell-edge UEs.

The convergence curves of TM and SA that apply HMs of  $\gamma_{c,5\%}^{(DL)}$  and  $\gamma_{c,50\%}^{(DL)}$  as optimization functions are shown in Figs. 9 and 10, respectively. In both figures, SA uses the best constant tilt equal to  $4^\circ$  as an initial solution, i.e.,  $\mathbf{x}_0 = 4^\circ \forall c$ , and is evaluated with two neighborhood structures  $N_A$  and  $N_B$ . According to the results, TM performs better than SA and achieves a noteworthy throughput gain when both approaches use the HM of  $\gamma_{c,50\%}^{(DL)}$  as an optimization function. Moreover, this throughput gain is achieved without any increase in computational complexity compared with SA.

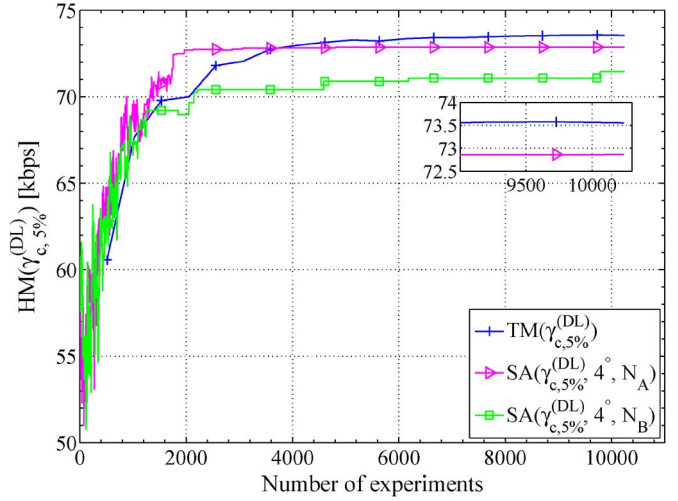


Fig. 9. HM of  $\gamma_{c,5\%}^{(DL)}$  as a function of the number of experiments for TM and SA indicated by  $SA(\gamma_{c,5\%}^{(DL)}, \mathbf{x}_0, \mathcal{N}(\mathbf{x}))$ , with  $\Theta_c$  as a configuration parameter.

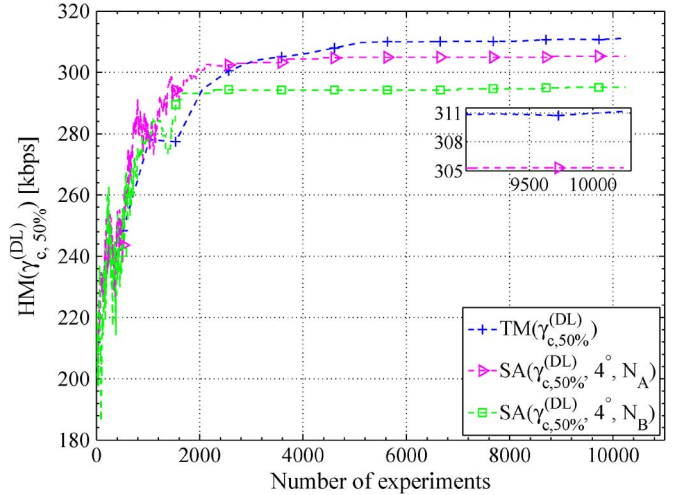


Fig. 10. HM of  $\gamma_{c,50\%}^{(DL)}$  as a function of the number of experiments for TM and SA indicated by  $SA(\gamma_{c,50\%}^{(DL)}, \mathbf{x}_0, \mathcal{N}(\mathbf{x}))$ , with  $\Theta_c$  as a configuration parameter.

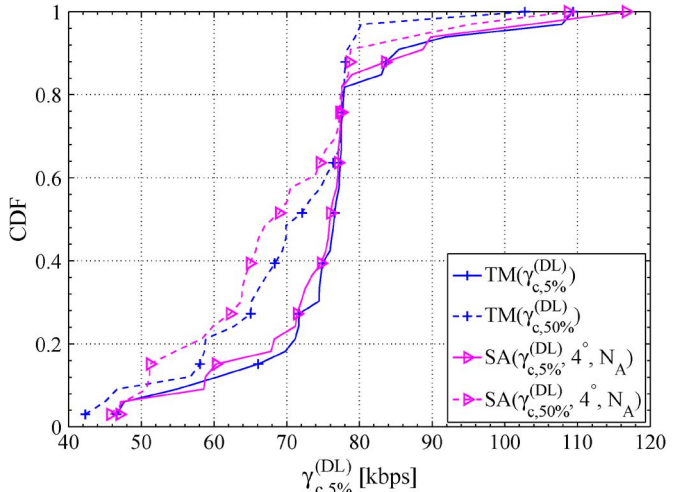


Fig. 11. CDFs of  $\gamma_{c,5\%}^{(DL)}$  obtained from applying TM and SA indicated by  $SA(\gamma_{c,p\%}^{(DL)}, \mathbf{x}_0, \mathcal{N}(\mathbf{x}))$ , with  $\Theta_c$  as a configuration parameter.

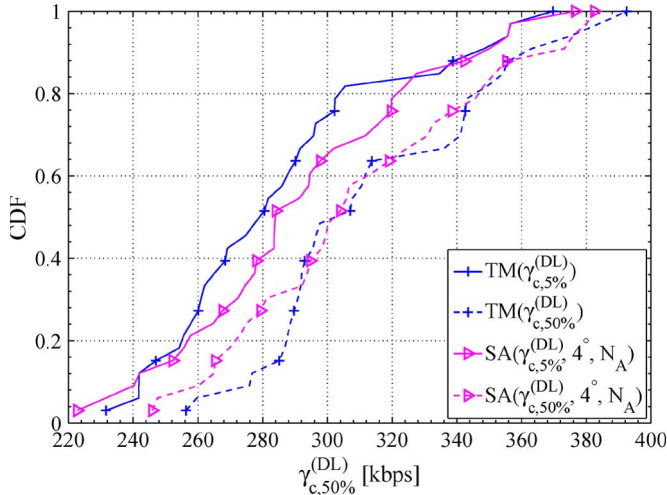


Fig. 12. CDFs of  $\gamma_{c,50\%}^{(DL)}$  obtained from applying TM and SA indicated by  $SA(\gamma_{c,p\%}^{(DL)}, \mathbf{x}_0, \mathcal{N}(\mathbf{x}))$ , with  $\Theta_c$  as a configuration parameter.

The CDF's of  $\gamma_{c,5\%}^{(DL)}$  are shown in Fig. 11 for TM and SA that apply the best neighborhood structure  $N_A$ . According to the figure, TM that applies the HM of  $\gamma_{c,5\%}^{(DL)}$  as an optimization function achieves a better performance than SA evaluated for the same metric. Note also that TM and SA that apply the HM of  $\gamma_{c,50\%}^{(DL)}$  as an optimization function have coverage performance degradation compared with approaches that apply  $\gamma_{c,5\%}^{(DL)}$ . This case is because the performance metric  $\gamma_{c,5\%}^{(DL)}$  maximizes the median UE throughput rather than the throughputs of the cell-edge UEs, as shown in Fig. 12. TM that applies the performance metric  $\gamma_{c,50\%}^{(DL)}$  achieves a notable increase in UE throughput compared with SA evaluated for the same metric. The minimum value of  $\gamma_{c,50\%}^{(DL)}$  has increased around 5%, and all the percentile values that are lower than 33 have improved.

**E. Optimization of the Antenna Azimuth Orientations in a Heterogeneous Network**

In a homogeneous network, where cells have the same properties such as coverage areas, the antenna azimuth orientations of a trisected eNodeB are typically set to the default values  $\Phi \in \{0^\circ, 120^\circ, -120^\circ\}$  referred to by a default setting. However, this setting would most likely not achieve the best performance in a heterogeneous network due to the irregular placement of the eNodeBs. In this section, the azimuth orientations of the eNodeBs' transmit antennas are subject to optimization by TM and SA.

The optimization should cover the full range of the azimuth orientation of one  $120^\circ$  sector of a trisected eNodeB. The maximum and minimum values of the azimuth orientation  $\Phi_c$  of the transmit antenna of sector  $c$  are determined by adding and subtracting  $59^\circ$  from its default setting, respectively. This case is illustrated in Fig. 13, which shows the optimization range for every transmit antenna of a single eNodeB. In addition, the impact of elevation is not considered, i.e.,  $h_{BS} = 0$  and  $\Theta_c = 0 \forall c$ . The optimized antenna azimuth orientations obtained by TM that applies the HM of  $\gamma_{c,50\%}^{(DL)}$  are shown in Fig. 2. It is

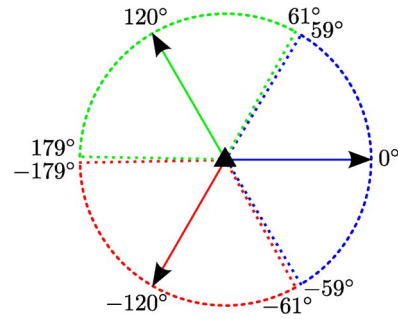


Fig. 13. Azimuth optimization range for each of the three transmit antennas of a single eNodeB.

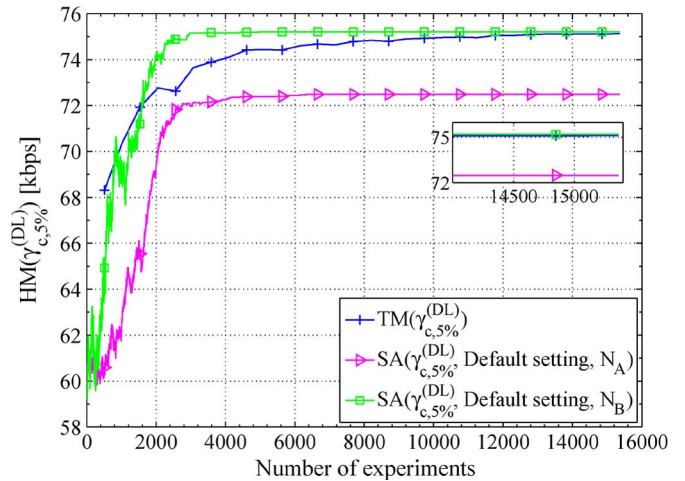


Fig. 14. HM of  $\gamma_{c,5\%}^{(DL)}$  as a function of the number of experiments for TM and SA indicated by  $SA(\gamma_{c,5\%}^{(DL)}, \mathbf{x}_0, \mathcal{N}(\mathbf{x}))$ , with  $\Phi_c$  as a configuration parameter.

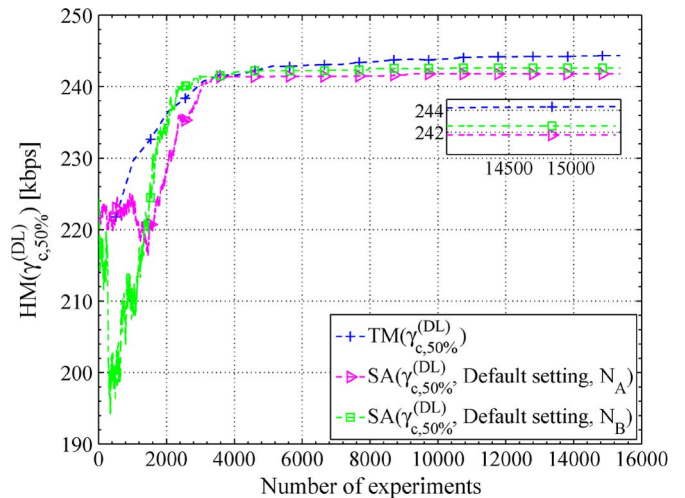


Fig. 15. HM of  $\gamma_{c,50\%}^{(DL)}$  as a function of the number of experiments for TM and SA indicated by  $SA(\gamma_{c,50\%}^{(DL)}, \mathbf{x}_0, \mathcal{N}(\mathbf{x}))$ , with  $\Phi_c$  as a configuration parameter.

shown that most of the optimized azimuth orientations deviate from the default settings.

The convergence curves of TM and SA that apply HMs of  $\gamma_{c,5\%}^{(DL)}$  and  $\gamma_{c,50\%}^{(DL)}$  are shown in Figs. 14 and 15, respectively. In both figures, SA uses the default setting as an initial solution and is evaluated with two neighborhood structures  $N_A$  and  $N_B$ . According to the figures, the neighborhood structure

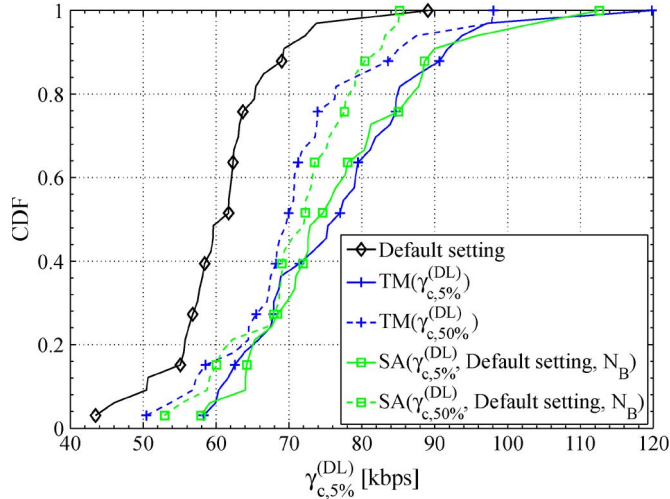


Fig. 16. CDFs of  $\gamma_{c,5\%}^{(DL)}$  obtained from applying TM and SA indicated by  $SA(\gamma_{c,p\%}^{(DL)}, \mathbf{x}_0, \mathcal{N}(\mathbf{x}))$ , with  $\Phi_c$  as a configuration parameter.

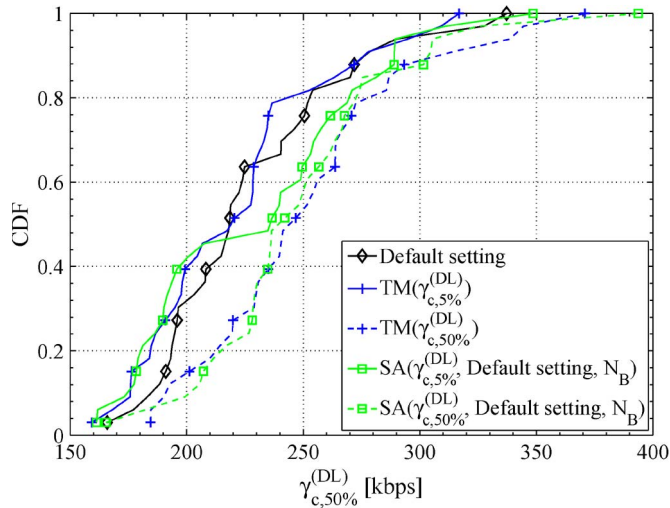


Fig. 17. CDFs of  $\gamma_{c,50\%}^{(DL)}$  obtained from applying TM and SA indicated by  $SA(\gamma_{c,p\%}^{(DL)}, \mathbf{x}_0, \mathcal{N}(\mathbf{x}))$ , with  $\Phi_c$  as a configuration parameter.

$N_B$  provides better performance than  $N_A$  in antenna azimuth optimization, whereas the latter structure yields better results than  $N_B$  in tilt optimization. Therefore, different neighborhood structures are needed for each optimization problem, rendering the performance of SA inconsistent. In Fig. 14, it is shown that SA that applies  $N_B$  and TM converge to the same value of the optimization function and outperform the SA that applies  $N_A$ . However, TM performs better than SA when both approaches apply the HM of  $\gamma_{c,50\%}^{(DL)}$  as an optimization function in Fig. 15.

The CDF's of  $\gamma_{c,5\%}^{(DL)}$  and  $\gamma_{c,50\%}^{(DL)}$  are shown in Figs. 16 and 17, respectively, for TM and the SA that applies the best neighborhood structure  $N_B$ . It can be observed that TM and SA have relatively comparable performance when both approaches are evaluated with the same optimization function. Moreover, TM and the SA that applies the HM of  $\gamma_{c,50\%}^{(DL)}$  have a degradation in coverage performance compared with approaches that apply the HM of  $\gamma_{c,5\%}^{(DL)}$ ; however, they still outperform the default setting.

## VII. CONCLUSION

The iterative optimization procedure based on TM has been a valuable means for radio network parameter optimization of a real-world heterogeneous network layout. Unlike the SA algorithm, which locally searches for new candidates in the neighborhood of the current parameter setting, TM explores a wider search space through the parameter combinations arranged by the OA, which refer to candidate solutions that are far apart from each other in the search space.

The definition of an optimization function that represents the network performance, which has been used to evaluate the experiments of TM, has a key role in steering the optimization toward cell coverage or capacity maximization. The optimization procedure based on TM has been illustrated for three use cases, where it successfully maximizes the function defined for network optimization. The use cases refer to the optimization of the following three typical cell-specific radio parameters of an LTE network: 1) the UL power control parameter  $P_{0,c}$ ; 2) the tilt of a transmit antenna, and 3) the azimuth orientation of a transmit antenna. Simulations have proved the good suitability of TM for radio network optimization. The results have shown that TM converges in most of the cases to values of the optimization function that are higher than the values achieved by the SA algorithm for the same complexity. Moreover, the performance of the SA algorithm considerably depends on the choice of the neighborhood structure as opposed to TM, which does not require a neighborhood definition and therefore provides a more stable and consistent operation in each optimization problem. Another advantage of TM is the decoupling of the number of parameters to be optimized and the computational complexity. This case is because the complexity of the algorithm is binded to the number of carried-out experiments determined by the OA rather than the number of configuration parameters.

Because TM allows any type of parameter combinations, it can also easily be extended to jointly optimize different cell-specific radio network parameters, e.g.,  $P_{0,c}$  in combination with a path-loss compensation coefficient  $\alpha_c$  or tilt in combination with azimuth orientation. For example, one straightforward way of jointly optimizing the antenna tilts and azimuths of  $k$  sectors is to build an OA with  $2 \cdot k$  columns and assign the antenna tilt parameters to the first  $k$  columns and the azimuth orientations to the rest. This approach, indeed, paves the way to exploit the mutual dependencies among the radio network parameters, achieve additional UE throughput gain, and reduce the computational complexity, because the parameters are simultaneously optimized. The joint optimization of the parameters will thoroughly be investigated in future work.

## REFERENCES

- [1] M. Rahnema, *UMTS Network Planning, Optimization and Interoperation With GSM*. Hoboken, NJ: Wiley, 2008.
- [2] S. Hurley, "Planning effective cellular mobile radio networks," *IEEE Trans. Veh. Technol.*, vol. 51, no. 2, pp. 243–253, Mar. 2002.
- [3] I. Siomina and D. Yuan, "Enhancing HSDPA performance via automated and large-scale optimization of radio base station antenna configuration," in *Proc. IEEE Veh. Technol. Conf.*, May 2008, pp. 2061–2065.
- [4] E. Almadi, A. Capone, F. Malucelli, and F. Signori, "UMTS radio planning: Optimizing base station configuration," in *Proc. IEEE Veh. Technol. Conf.*, Dec. 2002, vol. 2, pp. 768–772.

- [5] U. Turke and M. Koonert, "Advanced site configuration techniques for automatic UMTS radio network design," in *Proc. IEEE Veh. Technol. Conf.*, May 2005, vol. 3, pp. 1960–1964.
- [6] H. Meunier, E.-G. Talbi, and P. Reininger, "A multiobjective genetic algorithm for radio network optimization," in *Proc. Congr. Evol. Comput.*, Jul. 2000, vol. 1, pp. 317–324.
- [7] L. Goldstein and M. Waterman, "Neighborhood size in the simulated annealing algorithm," *Amer. J. Math. Manage. Sci.*, vol. 8, no. 3/4, pp. 409–423, Jan. 1988.
- [8] R. Roy, *A Primer on the Taguchi Method*. Dearborn, MI: Soc. Manuf. Eng., 1990.
- [9] G. Taguchi, "Taguchi methods in LSI fabrication process," in *Proc. IEEE Int. Workshop Stat. Methodology*, Jun. 2001, pp. 1–6.
- [10] G. Y. Hwang, S. M. Hwang, H. J. Lee, J. H. Kim, K. S. Hong, and W. Y. Lee, "Application of Taguchi method to robust design of acoustic performance in IMT-2000 mobile phones," *IEEE Trans. Magn.*, vol. 41, no. 5, pp. 1900–1903, May 2005.
- [11] S. R. Karnik, A. B. Raju, and M. S. Raviprakash, "Genetic-algorithm-based robust power system stabilizer design using Taguchi principle," in *Proc. 1st Int. Conf. Emerging Trends Eng. Technol.*, Jul. 2008, pp. 887–892.
- [12] H. Ikeda, T. Hanamoto, T. Tsuji, and M. Tomizuka, "Design of vibration suppression controller for 3-inertia systems using Taguchi method," in *Proc. Int. Symp. Power Electron., Elect. Drives, Autom. Motion*, 2006, pp. 1045–1050.
- [13] K. L. Virga and R. J. Engelhardt, Jr., "Efficient statistical analysis of microwave circuit performance using design of experiments," in *IEEE MTT-S Int. Microw. Symp. Dig.*, Jun. 1993, vol. 1, pp. 123–126.
- [14] Y. Cai and D. Liu, "Multiuser detection using the Taguchi method for DS-CDMA systems," *IEEE Trans. Wireless Commun.*, vol. 4, no. 4, pp. 1594–1607, Jul. 2005.
- [15] R. Roy, *Design of Experiments Using the Taguchi Approach: 16 Steps to Product and Process Improvement*. Hoboken, NJ: Wiley, 2001.
- [16] I. Viering, A. Lobinger, and S. Stefanski, "Efficient uplink modeling for dynamic system-level simulations of cellular and mobile networks," *EURASIP J. Wireless Commun. Netw.*, vol. 2010, pp. 1–15, Jul. 2010.
- [17] 3GPP, Further advancements for E-UTRA physical layer aspects, Sophia-Antipolis, France, 2009.
- [18] D. Henderson, S. H. Jacobson, and A. Johnson, *The Theory and Practice of Simulated Annealing*. Norwell, MA: Kluwer, 2003.
- [19] S. Kirkpatrick, C. D. Gelatt, and M. P. Vecchi, "Optimization by simulated annealing," *Science*, vol. 220, no. 4598, pp. 671–680, May 1983.
- [20] R. Mathar and T. Niessen, "Optimum positioning of base stations for cellular radio networks," *Wireless Netw.*, vol. 6, no. 6, pp. 421–428, Dec. 2000.
- [21] N. Pang, Y. You, and Y. Shi, "Application research on the simulated annealing in balance optimization of multiresource network planning," in *Proc. 2nd Int. Symp. IITA*, Dec. 2008, vol. 2, pp. 113–117.
- [22] W.-C. Weng, F. Yang, and A. Elsherbeni, "Linear antenna array synthesis using Taguchi's method: A novel optimization technique in electromagnetics," *IEEE Trans. Antennas Propag.*, vol. 55, no. 3, pp. 723–730, Mar. 2007.
- [23] A. S. Hedayat, N. Sloane, and J. Stufken, *Orthogonal Arrays: Theory and Applications*. New York: Springer-Verlag, 1999.
- [24] C. R. Rao, "Factorial experiments derivable from combinatorial arrangements of arrays," *J. R. Stat. Soc.*, vol. 9, no. 1, pp. 128–139, 1947.
- [25] N. J. A. Sloane, *A Library of Orthogonal Arrays*. [Online]. Available: <http://www2.research.att.com/~njas/oadir>
- [26] P. J. Ross, *Taguchi Techniques for Quality Engineering*. New York: McGraw-Hill, 1996.
- [27] I. Viering, M. Döttling, and A. Lobinger, "A mathematical perspective of self-optimizing wireless networks," in *Proc. IEEE Int. Conf. Commun.*, Jun. 2009, pp. 1–6.
- [28] J. Turkkka and A. Lobinger, "Nonregular layout for cellular network system simulations," in *Proc. IEEE Int. Symp. Pers., Indoor, Mobile Radio Commun.*, Sep. 2010, pp. 1929–1933.
- [29] 3GPP, "Physical layer aspects for Evolved UTRA," Sophia-Antipolis, France, TR 25.814, Tech. Rep., 2005.
- [30] R. Hoppe, "Comparison and evaluation of algorithms for the interpolation of 3-D antenna patterns based on 2-D horizontal and 2-D vertical patterns," AWE Commun. GmbH, Gärtringen, Germany, V 1.0, Tech. Rep., 2003.
- [31] 3GPP, "Evolved universal terrestrial radio access (E-UTRA) and evolved universal terrestrial radio access network (E-UTRAN): Overall description," Sophia-Antipolis, France, TS 36.300, Tech. Rep., 2009.
- [32] H. Holma and A. Toskala, *LTE for UMTS-OFMA and SC-FDMA Based Radio Access*. Hoboken, NJ: Wiley, 2009.
- [33] 3GPP, "Physical layer procedures," Sophia-Antipolis, France, TS 36.213, Tech. Rep., 2010.
- [34] B. Muhammad and A. Mohammed, "Performance evaluation of uplink closed loop power control for LTE system," in *Proc. IEEE Veh. Technol. Conf.*, 2009, pp. 1–5.
- [35] C. Castellanos, D. Villa, C. Rosa, K. Pedersen, F. Calabrese, P.-H. Michaelsen, and J. Michel, "Performance of uplink fractional power control in UTRAN LTE," in *Proc. IEEE Veh. Technol. Conf.*, 2008, pp. 2517–2521.
- [36] A. Simonsson and A. Furuskär, "Uplink power control in LTE—Overview and performance, principles and benefits of utilizing rather than compensating for SINR variations," in *Proc. IEEE Veh. Technol. Conf.*, 2008, pp. 1–5.
- [37] R. Mullner, C. Ball, K. Ivanov, J. Lienhart, and P. Hric, "Contrasting open-loop and closed-loop power control performance in UTRAN LTE uplink by UE trace analysis," in *Proc. IEEE Int. Conf. Commun.*, 2009, pp. 1–6.
- [38] P. Mogensen, W. Na, I. Kovacs, F. Frederiksen, A. Pokhariyal, K. Pedersen, T. Kolding, K. Hugel, and M. Kuusela, "LTE capacity compared to the Shannon bound," in *Proc. IEEE Veh. Technol. Conf.*, 2007, pp. 1234–1238.
- [39] B. E. Priyanto, T. B. Sorensen, and O. K. Jensen, "In-band interference effects on UTRA LTE uplink resource block allocation," in *Proc. IEEE Veh. Technol. Conf.*, 2008, pp. 1846–1850.



**Ahmad Awada** received the B.E. degree in computer and communications engineering from the American University of Beirut, Beirut, Lebanon, in 2007 and the M.S. degree in communication engineering from the Technical University of Munich, Munich, Germany, in 2009. He is currently pursuing the Ph.D. degree with the Department of Communications Technology, Darmstadt University of Technology, Darmstadt, Germany.

Since 2009, he has conducted his research activities with the Department of Radio Systems, Nokia Siemens Networks, Germany. His research interests include self-organizing networks and network optimization processes.



**Bernhard Wegmann** received the Dipl.-Ing. and Dr. Ing. (Ph.D.) degrees in communications engineering from the Technical University of Munich, Munich, Germany, in 1987 and 1993, respectively.

In 1995, he joined the Communications Group, Siemens AG, where he has worked in different departments as an R&D, Standardization, Strategic Product Management, and Network Engineer. Along with the merger of the Communication Group, Siemens AG, and the Network Group, Nokia, in April 2007, he moved to Nokia Siemens Networks, where he is currently with the research group for future mobile radio systems, dealing with Long-Term Evolution (LTE) and LTE-A standardization research. His research interests include radio transmission techniques, radio resource management, self-organizing networks, and radio network deployment.



**Ingo Viering** (M'09) received the Dipl.-Ing. degree from Darmstadt University of Technology, Darmstadt, Germany, in 1999 and the Dr. Ing. degree from the University of Ulm, Ulm, Germany, in 2003.

In 2002, he spent a research stay with the Telecommunications Research Center Vienna (FTW), Vienna, Austria, where he conducted early measurements of the multiple-input-multiple-output channel. He is a Cofounder and the Acting Chief Executive Officer of Nomor Research GmbH, Munich, Germany. Before founding Nomor Research in 2004, he was with Siemens as a Consultant in all air-interface-related research areas. Among others, he supervised collaborations with universities, backofficed Third-Generation Partnership Project standardization, and was involved in the early evaluation of emerging technologies such as Flash-orthogonal frequency-division multiplexing, WiMAX, and Long-Term Evolution. Since 2007, he has been a Senior Lecturer with the Technical University of Munich, Munich, Germany. He is the holder of around 60 pending patents and has published more than 40 scientific papers.

Dr. Viering received the 2009 VDE Award for the achievements of Nomor Research.



**Anja Klein** (M'95) received the Diploma and Dr. Ing. (Ph.D.) degrees in electrical engineering from the University of Kaiserslautern, Kaiserslautern, Germany, in 1991 and 1996, respectively.

From 1991 to 1996, she was a member of Staff with the Research Group for RF Communications, University of Kaiserslautern. In 1996, she joined the Mobile Networks Division, Siemens AG, Munich and Berlin, Germany. She was active in the standardization of third-generation mobile radio in the European Telecommunications Standards Institute and the Third-Generation Partnership Project (3GPP), for example, leading the TDD Group, RAN1, 3GPP. She was a Vice President, heading a development department and a systems engineering department. In May 2004, she joined the Technische Universität Darmstadt, Darmstadt, Germany, as a Full Professor, heading the Communications Engineering Laboratory. She has published more than 150 refereed papers and has contributed to five books. She is the inventor and co-inventor of more than 45 patents in mobile radio. Her research interests include mobile radio, in particular multiple access, single-carrier and multicarrier transmission schemes, multiantenna systems, radio resource management, network planning and dimensioning, relaying, and cooperative communications.

Dr. Klein is a member of the Verband Deutscher Elektrotechniker–Informationstechnische Gesellschaft. She received the Inventor of the Year Award from Siemens AG in 1999.